Synthesis and Structures of Coordination Polymers with 4,4′-Dipyridyldisulfide

Mitsuru Kondo,* Mariko Shimamura,† Shin-ichiro Noro,† Yu Kimura,*
Kazuhiro Uemura,* and Susumu Kitagawa*,1

*Department of Synthetic Chemistry and Biological Chemistry, Graduate School of Engineering, Kyoto University, Yoshida, Sakyo-ku, Kyoto 606-8501, Japan;
and †Department of Chemistry, Graduate School of Science, Tokyo Metropolitan University, 1-1 Minamiohsawa, Hachioji-shi, Tokyo 192-0397, Japan

Two new coordination compounds, [Mn(bpe)$_2$(NCS)$_2$] (bpe, 4,4′-bipyridylethane) (1) and [Cd(dpds)$_2$(H$_2$O)$_2$]·2NO$_3$·2EtOH· 2H$_2$O (dpds, 4,4′-dipyridyldisulfide) (2·2EtOH·2H$_2$O), were synthesized and structurally characterized. 1 crystallizes in the monoclinic space group *C2/c* (No.15) with $a = 19.928(3)$ Å, $b = 10.060(3)$ Å, $c = 14.680(3)$, $\beta = 110.30(1)°$, $V = 2760.1(9)$ Å^3, and $Z = 4$. 2·2EtOH·2H$_2$O crystallizes in the monoclinic space group *P2$_1$/n* (No. 14) with $a = 8.9735(9)$, $b = 19.835(1)$, $c = 10.778(2)$, $\beta = 112.29(1)°$, $V = 1775.1(1)$ Å^3, and $Z = 2$. 1 has an elongated octahedral manganese center with the two NCS$^-$ anions in the axial sites, while 2·2EtOH·2H$_2$O provides a distorted octahedral center with water molecules in the axial sites. For both compounds, the basal plane is filled with the four pyridine donors. Each metal ion in these compounds is linked by the two bridging ligands to make up a one-dimensional structure with large cavities. Assembled structures of these compounds contain 3×2 Å and 5×4 Å of microchannels for 1 and 2·2EtOH·2H$_2$O, respectively. Although the channels of 2·2EtOH·2H$_2$O have enough dimension for small molecules, the dried compound shows no methane adsorption property because this pore structure is not retained after removal of the guest molecules. On the other hand, the network of 2 demonstrates unique redox property in solid state. A cyclic voltammogram of this compound reveals redox activity, which is ascribed to the reduction of the disulfide bond to thiolate and reoxidation of the thiolate to disulfide. The redox activity of the coordination polymer shows a new class of network material. © 2000 Academic Press

Key Words: redox active coordination network; porous structure; 4,4′-dipyridyldisulfide; 4,4′-bipyridylethane; one-dimensional structure; self-assembled network.

INTRODUCTION

Design and construction of coordination networks with unique functions are a great challenge in the field of network materials (1–10). Much effort has been devoted to modifing the building units and to controlling the assembled motifs and the unique functions such as molecular magnets (9, 11) electric conductors (12), or the zeolite-like porous materials (3, 7, 13–15). We have obtained various coordination networks from bis(pyridine)-type ligands, for example, pyrazine, 4,4′-bipyridine (16, 17), pyrazine-2,3-dicarboxylate (18), 1,4-bis(4-pyridoxy)benzene (bpob) (19), 4,4′-azopyridine (azpy) (20, 21), and N-(4-pyridyl)isonicotinamide (pia) (18, 22). It has been demonstrated that their structures and functions are directed by the type of bridging ligands.

Recently we have studied redox properties of the bridging ligand azpy in the coordination networks of {[Fe(azpy) (NCS)$_2$(MeOH)$_2$]·azpy} and [Fe(azpy)$_2$(NCS)$_2$] (21). The azpy ligand held by hydrogen bonding shows a redox reaction similar to that of the free azpy molecule, while the azpy ligand directly binds to the iron atom and shows no redox properties. This fact indicates the restriction of the coordination network on the redox activities of bridging ligands.

In addition to the ligand, we selected 4,4′-dipyridyldisulfide (dpds) (Scheme 1) in this work for the creation of a new functional coordination network that could yield a redox active framework and have succeeded in the synthesis and characterization of a new coordination polymer, [Cd(dpds)$_2$(H$_2$O)$_2$]·2NO$_3$·2EtOH·2H$_2$O. Although a skeleton of dpds is similar to that of 4,4′-bipyridylethane (bpe), the network structures obtained by the combination with cadmium nitrate are quite different; it has been reported that the cadmium nitrate with bpe yields a one-dimensional compound, [Cd$_2$(bpe)$_3$(NO$_3$)$_4$], with a T-shaped metal center (23). In order to study the effect of disulfide moiety on network topology, the new coordination polymer, [Mn(bpe)$_2$ (NCS)$_2$], was also synthesized and crystallographically characterized. In this paper, structures and functions of a coordination network with dpds ligand are described.

EXPERIMENTAL

Synthesis of [Mn(bpe)$_2$(NCS)$_2$] (**1**). An ethanol solution (20 mL) of bpe (0.76 g, 4.1 mmol) was slowly diffused into an

---
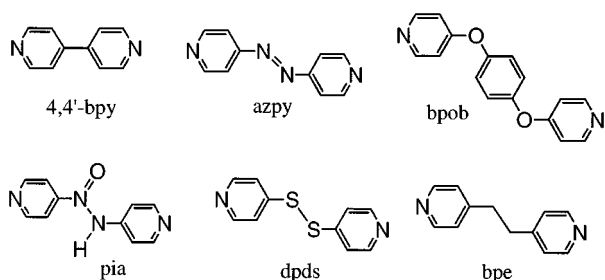
SCHEME 1

aqueous solution (20 mL) of $MnCl_2 \cdot 6H_2O$ (0.43 g, 1.8 mmol) and NH_4SCN (0.32 g, 4.2 mmol). White brick crystals were obtained in 1 week. One of them was used for X-ray analysis. The residual crystals were collected by filtration and dried *in vacuo*. Yield, 0.68 g (1.3 mmol, 72%); Anal. Calcd for $C_{26}H_{24}MnN_6S_2$: C, 57.87; H, 4.48; N, 15.57; Found: C, 57.95; H, 4.51; N, 15.28.

Synthesis of [Cd(dpds)₂(H₂O)₂] · 2NO₃ (**2**). An aqueous solution (15 mL) of $Cd(NO_3)_2 \cdot 4H_2O$ (0.24 g, 0.78 mmol) in H_2O was slowly diffused into an ethanol solution (15 mL) of dpds (0.488 g, 2.2 mmol). White plate crystals of $2 \cdot 2EtOH \cdot 2H_2O$ were formed in 1 week. One of them was used for X-ray analysis, and the residual crystals were collected by filtration, washed with H_2O and EtOH, and dried *in vacuo*. Although the single-crystal structure involves guest ethanol and water molecules, solvent molecules were lost during the drying process. Anal. Calcd for $C_{20}H_{20}CdN_6O_8S_4$: C, 33.69; H, 2.83; N, 11.79. Found: C, 32.69; H, 2.52; N, 10.74.

Physical measurements. X-ray powder diffraction data were collected on a MAC Science MXP18 automated diffractometer by using $CuK\alpha$ radiation. A cyclic voltammogram (CV) was taken on a BAS CV-50W polarographic analyzer according to the described in the literature method (21, 24). A SCE electrode was used as a reference. Each bulk sample of free dpds or **2** was added to carbon paste (graphite and mineral oil) and mixed well. By using this mixture a working electrode was prepared: platinum wire. Another platinum wire was used as a counter electrode. Three-electrode system was employed in $0.1 \, mol \, dm^{-3}$ $NaClO_4$ aqueous solution, using a scan rate of $10 \, mV \, s^{-1}$ in the range -1.2 to 1.2 V.

X-ray structure determination. For each compound, a suitable crystal was sealed in a glass capillary. For **1** data collections were carried out on a Rigaku AFC7R diffractometer with a monochromatic $MoK\alpha$ radiation source ($\lambda = 0.71069$ Å). Unit-cell constants were obtained from a least-squares refinement using the setting angles of 25 well-centered reflections in the ranges $25.22 < 2\theta < 29.89°$. Crystallographic data are given in Table 1. An empirical absorption correction based on azimuthal scans of several

reflections was applied. The data were corrected for Lorentz and polarization effects.

For $2 \cdot 2EtOH \cdot 2H_2O$, X-ray data collection was carried out by an oscillation method using a Rigaku R-AXIS IV imaging-plate system on a rotating-anode X-ray generator operated at 50 kV, 100 mA. Crystallographic data are given in Table 1. Laue group and unit-cell parameters were determined by data-processing software (*PROCESS*) attached to the R-AXIS system. Lorentz and polarization corrections were applied.

The structures were solved by a direct method and expanded using Fourier techniques. The nonhydrogen atoms were refined anisotropically. Hydrogen atoms were placed in idealized positions and were included but not refined. The refinements were carried out using full-matrix least-squares techniques. All calculations were performed using the *TEXSAN* crystallographic software package of Molecular Structure Corporation. The final fractional atomic coordinates and selected bond distances for **1** and $2 \cdot 2EtOH \cdot 2H_2O$ are listed in Tables 2 and 3, respectively.

RESULTS AND DISCUSSION

Structure of **1**. Figure 1a shows the ORTEP drawing of manganese center of **1** with a numbering scheme, where the

TABLE 1
Crystallographic Data for [Mn(bpe)₂(NCS)₂] (1) and [Cd(dpds)₂(H₂O)₂]·2NO₃·2EtOH·2H₂O (2·2EtOH·2H₂O)

	1	**2·2EtOH·2H₂O**
Empirical formula	$C_{26}H_{24}MnN_6S_2$	$C_{24}H_{36}CdN_6O_{12}S_4$
Formula weight	539.57	841.23
Crystal system	Monoclinic	Monoclinic
a (Å)	19.928(3)	8.9735(9)
b (Å)	10.060(3)	19.835(1)
c (Å)	14.680(3)	10.778(2)
β (°)	110.30(1)	112.29(1)
V (Å³)	2760.1(9)	1775.1(4)
Z	4	2
Space group	$C2/c$ (No. 15)	$P2_1/n$ (No. 14)
T (°C)	23	23
λ (MoKα) (Å)	0.71069	0.71069
ρ_{calc} (g/cm³)	1.298	1.574
μ (cm⁻¹)	6.54	9.15
θ range (°)	$6.0 < 2\theta < 55.0$	$6.0 < 2\theta < 55.0$
Reflection measured	3450	3166
Independent reflections	3353	2626
R_{int}	0.022	0.0625
Used in refinement	1282 ($I > 2\sigma(I)$)	2626 ($I > 3\sigma(I)$)
Variables	160	214
R^a	0.045	0.049
$R_w{}^b$	0.047	0.053
S	1.29	1.78

$^a R = \sum ||Fo| - |Fc|| / \sum |Fo|$.
$^b R_w = [(\sum_w(|Fo| - |Fc|)^2 / \sum_w Fo^2)]^{1/2}$.

TABLE 2
Atomic Coordinates ($\times 10^4$) and Equivalent Isotropic Thermal Parameters ($\mathring{A}^2$) for [Mn(bpe)$_2$(NCS)$_2$] (1)

Atom	x	y	z	$U_{eq}{}^a$
Mn(1)	0.5000	0.0050(1)	0.2500	0.0446(3)
S(1)	0.28814(8)	−0.0820(2)	0.3244(1)	0.0734(6)
N(1)	0.4412(2)	0.1694(4)	0.1437(3)	0.049(1)
N(2)	0.4313(2)	0.8446(4)	0.1488(3)	0.050(1)
N(3)	0.4205(2)	−0.0019(5)	0.3214(3)	0.061(1)
C(1)	0.3754(3)	0.2094(5)	0.1341(4)	0.056(2)
C(2)	0.3379(3)	0.3024(5)	0.0675(4)	0.056(2)
C(3)	0.3680(3)	0.3598(5)	0.0052(4)	0.048(2)
C(4)	0.4364(3)	0.3213(6)	0.0174(4)	0.067(2)
C(5)	0.4703(3)	0.2284(6)	0.0859(4)	0.071(2)
C(6)	0.4109(3)	0.8545(5)	0.0519(4)	0.056(2)
C(7)	0.3638(3)	0.7681(5)	−0.0119(3)	0.053(2)
C(8)	0.3363(3)	0.6632(5)	0.0241(4)	0.047(2)
C(9)	0.3568(3)	0.6516(5)	0.1241(4)	0.053(2)
C(10)	0.4034(3)	0.7420(5)	0.1817(3)	0.054(2)
C(11)	0.3267(3)	0.4543(5)	−0.0746(4)	0.060(2)
C(12)	0.2860(3)	0.5643(5)	−0.0433(4)	0.059(2)
C(13)	0.3654(3)	−0.0346(4)	0.3227(3)	0.045(2)
H(1)	0.3532	0.1719	0.1762	0.0679
H(2)	0.2913	0.3277	0.0644	0.0670
H(3)	0.4605	0.3591	−0.0217	0.0815
H(4)	0.5180	0.2048	0.0924	0.0858
H(5)	0.4300	0.9250	0.0257	0.0670
H(6)	0.3505	0.7810	−0.0799	0.0649
H(7)	0.3384	0.5818	0.1522	0.0635
H(8)	0.4170	0.7312	0.2500	0.0642
H(9)	0.3593	0.4951	−0.0998	0.0695
H(10)	0.2926	0.4040	−0.1240	0.0695
H(11)	0.2574	0.5257	−0.0105	0.0692
H(12)	0.2565	0.6103	−0.0992	0.0692

$^a U_{eq} = 1/3\,[U1 + U2 + U3]$.

metal sites are in the crystallographic twofold axis. Selected bond distances and angles are listed in Table 4. The manganese has a distorted elongated octahedral environment with two thiocyanate nitrogen donors in the axial sites and four pyridine nitrogen donors in the basal plane. The pyridine rings are arranged in a propeller fashion around the equatorial plane. The *trans* N–Mn–N bond angles for NCS and pyridine ligands are 176.4(3)° and 174.1(2)°, respectively. The *cis* N–Mn–N bond angles range from 85° to 94°, indicative of a distorted octahedral environment. The NCS ligands are coordinated to the manganese atom in a bent fashion with the angle C(13)–N(3)–Mn(1) of 150.7(4)°. The NCS ligand itself is almost linear; the N(3)–C(13)–S(1) is 179.5(5)°.

Each manganese atom is linked by two bpe ligands to afford a one-dimensional framework along the *b* axis (Fig. 1b). The chain framework contains large cavities (about $4 \times 4\ \mathring{A}$) formed by two manganese atoms and two bpe ligands, in which the nonbonded distance between the two manganese atoms is about 10.1 Å. The torsion angle of the (CH$_2$–CH$_2$) moiety, i.e., C(3)–C(11)–C(12)–C(8), is 68.4(6)°, which is close to the value (60°) expected for the gauche-staggered conformation of the methylene bond.

Although there are no direct bondings between the chains, these are regularly assembled to yield small size channels (about $3 \times 2\ \mathring{A}$), which contain no guest molecules, along the *a* axis as shown in Fig. 1c, whose porosity of this compound is comparable to some zeolite materials, i.e., analcime (about $2 \times 2\ \mathring{A}$), natrolite, or thomsonite (about $3 \times 4\ \mathring{A}$). This size of channel could adsorb water molecules, but is too small to adsorb usual guest molecules. Actually, this compound shows no effective methane adsorption property at a pressure range 1 to 36 atm at room temperature.

TABLE 3
Atomic Coordinates ($\times 10^4$) and Equivalent Isotropic Thermal Parameters ($\mathring{A}^2$) for [Cd(dpds)$_2$(H$_2$O)$_2$]·2NO$_3$·2EtOH·2H$_2$O (2·2EtOH·2H$_2$O)

Atom	x	y	z	$U_{eq}{}^a$
Cd(1)	1.0000	0.0000	1.0000	0.0277(1)
S(1)	1.4133(1)	−0.24060(5)	1.4705(1)	0.0358(3)
S(2)	1.6513(1)	−0.23634(5)	1.5022(1)	0.0362(3)
O(1)	0.7800(3)	−0.0139(1)	1.0714(3)	0.0401(8)
O(2)	0.5739(5)	−0.1220(2)	1.0125(4)	0.079(1)
O(3)	0.5487(5)	−0.2299(2)	1.0195(4)	0.073(1)
O(4)	0.7254(5)	−0.1761(2)	1.1851(4)	0.078(1)
O(5)	0.3113(5)	−0.0475(2)	0.7441(4)	0.087(2)
O(6)	0.8120(4)	−0.3187(2)	1.2640(4)	0.078(1)
N(1)	1.1491(4)	−0.0859(2)	1.1484(4)	0.0344(9)
N(2)	1.8784(4)	−0.0808(2)	1.8327(3)	0.0312(9)
N(3)	0.6159(5)	−0.1765(2)	1.0719(4)	0.054(1)
C(1)	1.3076(5)	−0.0964(2)	1.1811(4)	0.036(1)
C(2)	1.3960(5)	−0.1420(2)	1.2758(4)	0.035(1)
C(3)	1.3197(5)	−0.1797(2)	1.3445(4)	0.0284(10)
C(4)	1.1551(5)	−0.1703(2)	1.3085(5)	0.038(1)
C(5)	1.0775(5)	−0.1232(2)	1.2137(5)	0.039(1)
C(6)	1.7178(5)	−0.0895(2)	1.7803(4)	0.036(1)
C(7)	1.6415(5)	−0.1358(2)	1.6840(4)	0.037(1)
C(8)	1.7321(5)	−0.1749(2)	1.6299(4)	0.0286(10)
C(9)	1.8981(5)	−0.1656(2)	1.6817(4)	0.034(1)
C(10)	1.9637(5)	−0.1194(2)	1.7826(5)	0.035(1)
C(11)	0.282(1)	0.0041(4)	0.547(1)	0.218(5)
C(12)	0.212(1)	−0.0328(5)	0.620(1)	0.203(5)
H(1)	1.3613	−0.0717	1.1304	0.0361
H(2)	1.5093	−0.1479	1.2930	0.0364
H(3)	1.0966	−0.1944	1.3562	0.0401
H(4)	0.9673	−0.1139	1.1942	0.0425
H(5)	1.6523	−0.0616	1.8154	0.0396
H(6)	1.5293	−0.1424	1.6539	0.0401
H(7)	1.9651	−0.1904	1.6434	0.0359
H(8)	2.0783	−0.1114	1.8165	0.0361
H(9)	0.1925	0.0107	0.4553	0.1312
H(10)	0.3504	−0.0290	0.5293	0.1312
H(11)	0.3248	0.0410	0.5820	0.1312
H(12)	0.1543	−0.0682	0.5712	0.1705
H(13)	0.1288	0.0019	0.6239	0.1705

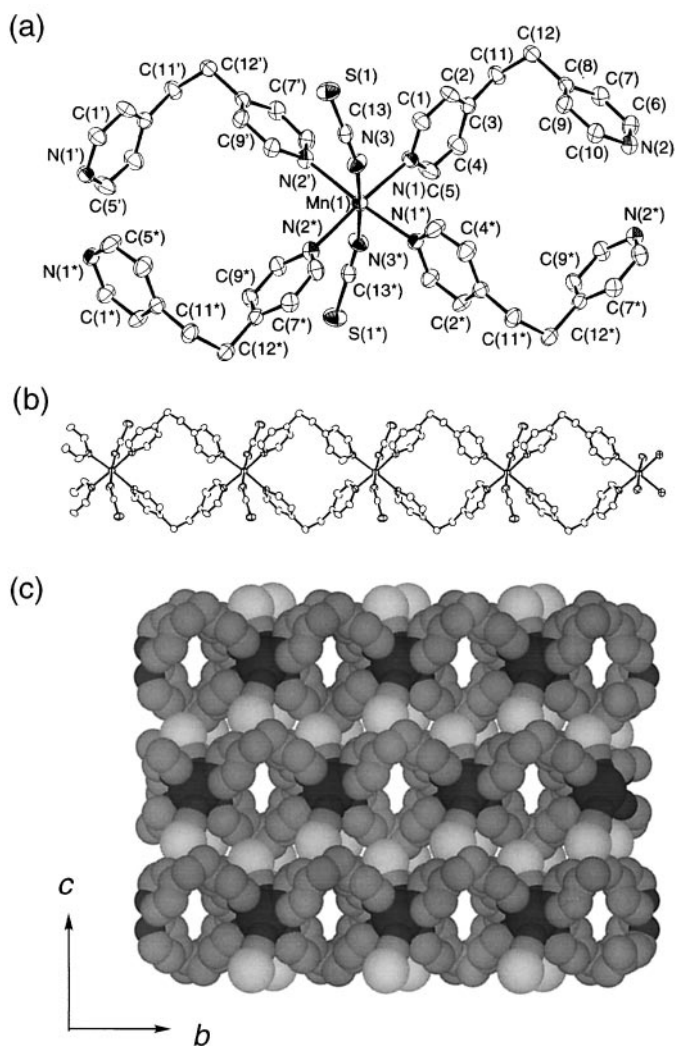$^a U_{eq} = 1/3\,[U1 + U2 + U3]$.

FIG. 1. ORTEP drawing of the manganese center of **1** with the non-hydrogen atoms at the 30% probability level (a). View of the one-dimensional structure (b). A space-filling model of **1** with the nonhydrogen atoms along the *a* axis, indicating the aspects of the 3 × 2 Å channel structure (c).

Structure of **2**·*2EtOH·2H*₂*O.* Figure 2a shows the ORTEP drawing of the cadmium center of **2**·2EtOH·2H₂O with a numbering scheme, where the metal sites are in the crystallographic inversion center. Selected bond distances and angles are listed in Table 4. The cadmium has a distorted elongated octahedral environment with two water oxygens in the axial sites and four pyridine nitrogen donors in the basal plane. The *trans* N–Cd–N and O–Cd–O bond angles are crystallographically 180°. On the other hand, *cis* N–Cd–O and N–Cd–N bond angles range from 88° to 92°, indicative of distorted octahedral environment.

Each cadmium center is bridged by two dpds ligands to form a one-dimensional framework along the (*a* + *c*) vector. The nonbonded distance between the cadmium centers is about 11.1 Å. Although this network motif is similar to that

of **1**, the framework structure is slightly different. The torsion angle formed by the disulfide moiety, i.e., C(4)–S(1)–S(2)–C(8), is about 90°, whose value is close to that of the usual disulfide normal for the sulfide compounds. The cavity framework defined by two dpds ligands and two cadmium atoms has a crystallographic inversion center.

The assembled structure of this compound shows a clear difference from that of **1** in the channels (about 5 × 4 Å), which run along the *a* axis and are filled with guest ethanol molecules. Oxygen atoms of the ethanol molecules and nitrate counter anions are hydrogen bonded to the co-ordinating water molecules (O(1)–O(5*) = 2.710(6) Å). Nitrate anions are not included in the channel-like cavities but are positioned above or below the one-dimensional chains without blocking the channels. To the best of our knowledge, this is the first example of the well-characterized coordination network of dpds ligands.

The single-crystal X-ray diffraction study clearly demonstrates that the reaction of dpds with cadmium nitrate yields crystals of a product that was formulated as [Cd(dpds)₂(H₂O)₂]·2NO₃·2EtOH·2H₂O. The uncoordinated ethanol and water molecules could be removed under reduced pressure; the dried compound is formulated as [Cd(dpds)₂(H₂O)₂]·2NO₃ by elemental analysis.

Function of dpds network. Although the single-crystal X-ray diffraction study clearly demonstrates that the crystals

TABLE 4
Selected Bond Distances and Angles of [Mn(bpe)₂(NCS)₂] (1) and [Cd(dpds)₂(H₂O)₂]·2NO₃·2EtOH·2H₂O(2·2EtOH·2H₂O)

Compound **1**							
Mn(1)	N(1)	2.296(4)		Mn(1)	N(2)	2.297(4)	
Mn(1)	N(3)	2.183(4)					
N(1)	Mn(1)	N(1)	87.9(2)	N(1)	Mn(1)	N(2)	91.0(1)
N(1)	Mn(1)	N(2)	174.1(1)	N(1)	Mn(1)	N(3)	93.7(2)
N(1)	Mn(1)	N(3)	88.9(2)	N(1)	Mn(1)	N(2)	174.1(1)
N(1)	Mn(1)	N(2)	91.0(1)	N(1)	Mn(1)	N(3)	88.9(2)
N(1)	Mn(1)	N(3)	93.7(2)	N(2)	Mn(1)	N(2)	90.7(2)
N(2)	Mn(1)	N(3)	85.3(2)	N(2)	Mn(1)	N(3)	92.1(2)
N(2)	Mn(1)	N(3)	92.1(2)	N(2)	Mn(1)	N(3)	85.3(2)
N(3)	Mn(1)	N(3)	176.3(3)	Mn(1)	N(1)	C(1)	122.7(3)
Compound **2**·2EtOH·2H₂O							
Cd(1)	O(1)	2.391(3)		Cd(1)	N(1)	2.373(3)	
Cd(1)	N(2)	2.349(3)		S(1)	S(2)	2.033(2)	
O(1)	Cd(1)	O(1)	180.0	O(1)	Cd(1)	N(1)	91.4(1)
O(1)	Cd(1)	N(1)	88.6(1)	O(1)	Cd(1)	N(2)	88.2(1)
O(1)	Cd(1)	N(2)	91.8(1)	O(1)	Cd(1)	N(1)	88.6(1)
O(1)	Cd(1)	N(1)	91.4(1)	O(1)	Cd(1)	N(2)	91.8(1)
O(1)	Cd(1)	N(2)	88.2(1)	N(1)	Cd(1)	N(1)	180.0
N(1)	Cd(1)	N(2)	90.4(1)	N(1)	Cd(1)	N(2)	89.6(1)
N(1)	Cd(1)	N(2)	89.6(1)	N(1)	Cd(1)	N(2)	90.4(1)
N(2)	Cd(1)	N(2)	180.0	S(2)	S(1)	C(3)	105.2(2)
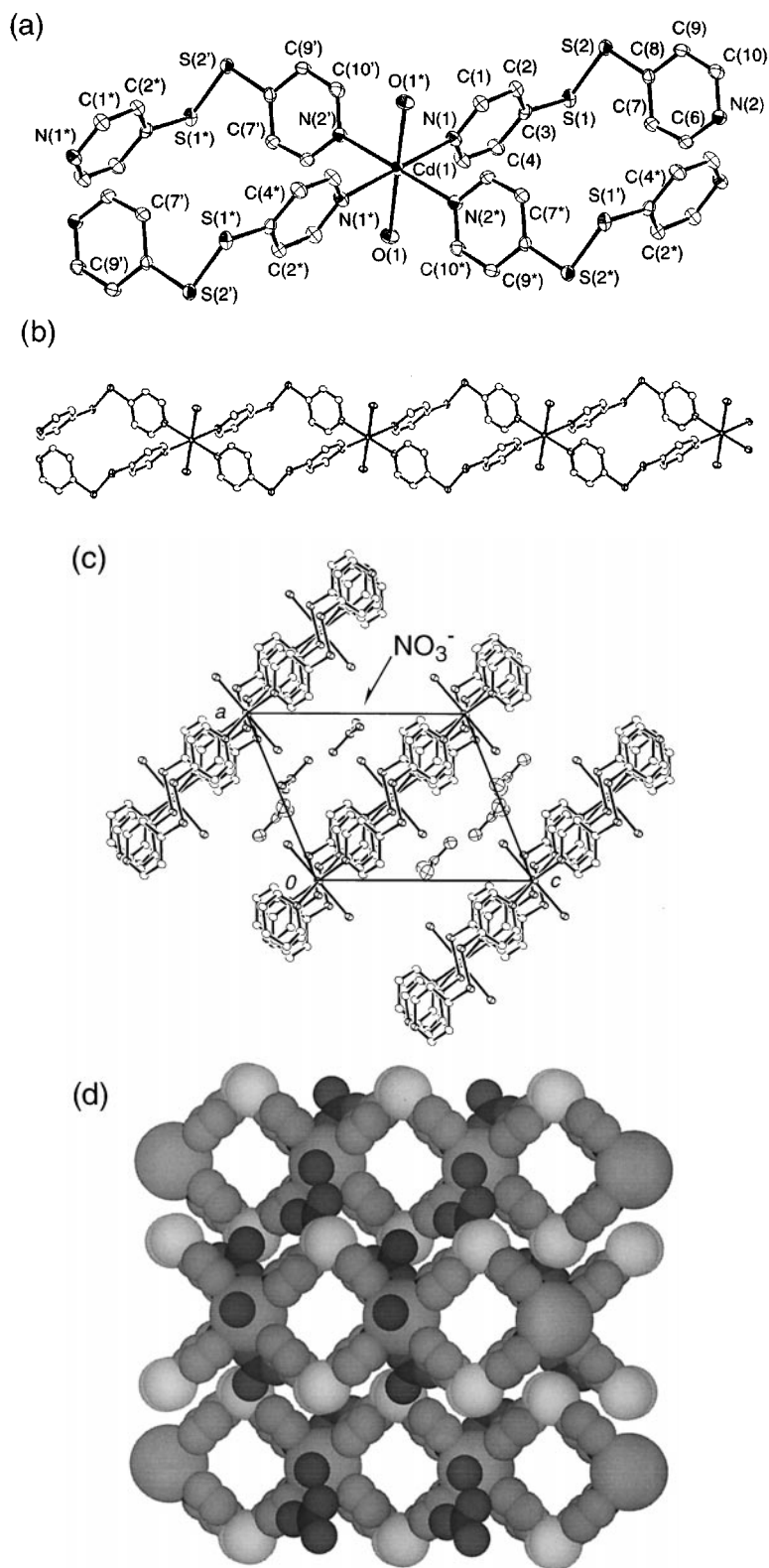
FIG. 2. ORTEP drawing of the cadmium center of **2**·2EtOH·2H$_2$O with the non-hydrogen atoms at the 30% probability level (a). View of the one-dimensional structure (b). The projection view along the *b*-axis (c). The channel structure (d). A space-filling model of **2**·2EtOH·2H$_2$O with the nonhydrogen atoms along the *a* axis, indicating the formation of large size (5 × 4 Å) of channels. Guest ethanol and water molecules are omitted for clarity.

of the product $2 \cdot 2EtOH \cdot 2H_2O$ form channels with a dimension of 5×4 Å, we have demonstrated that such channels reversibly adsorb large amounts of gas molecules under high pressure at room temperature when the network is tightly held (16, 18). However, the dried compound **2** does not show an appreciable gas adsorption property because of the phase transition, coupled with the deformation of the porous structure, upon removal of the included guest molecules. These findings were confirmed by the measurements of X-ray powder diffraction (XRPD) pattern of the dried compound. Figure 3 illustrates the observed XRPD patterns of **1** and dried compound **2** with their simulated patterns obtained from the single-crystal models. In the case of **1**, the observed XRPD pattern shows a good agreement with the simulated pattern, while the peak positions and the pattern observed for **2** are apparently different from those of the simulated pattern.

Although detailed structure is unknown, intense and sharp XRPD diffraction of **2** implies the formation of a new assembled phase of its one-dimensional chains. The redox activity of the dpds moiety incorporated in the network was estimated by using a CV measurement in the solid state. Figure 4 shows the CV charts of **2** and free dpds, which were measured for comparison. Free dpds shows redox waves at -1.1 and 0.3 V (vs SCE), which are ascribed to reduction of the disulfide bond to thiolate anions and reoxidation to disulfide, respectively (Eq. 1).

$$py{-}S{-}S{-}py + 2\,e^- \rightleftharpoons 2\,py{-}S^-. \qquad [1]$$
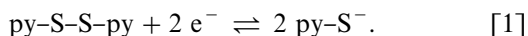
2 shows the corresponding redox waves at -1.2 and 1.0 V. The potentials slightly shift compared with those of the free dpds. Moreover, the reduction wave is sharper than that of the free dpds, and the wave corresponding to the reoxidation to disulfide is quite small. These aspects are likely due to the effect of the restriction of the network on the redox property.

We have prepared the coordination networks with azpy ligands, $\{[Fe(azpy)(NCS)_2(MeOH)_2]\cdot azpy\}$ and $[Fe(azpy)_2 (NCS)_2]$ (21). The azo group is also a redox active moiety, whose mechanism is represented by Eq. 2.

$$py{-}N{=}N{-}py + 2\,e^- + 2\,H^+ \rightleftharpoons py{-}NH{-}NH{-}py. \qquad [2]$$
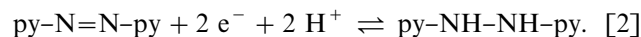
The two types of azpy ligands are found in these network materials, i.e., one is directly bonded to the iron center and the other is associated by hydrogen bonds. The hydrogen-bonded azpy ligands are redox active in the solid state, while the azpy ligands that directly bind to the iron centers are not redox active in the range 1.2 to -1.2 V (vs SCE). In contrast with the case of the azpy ligand, dpds ligand undergoes reduction at the potential close to that of free dpds even when the ligand is tightly incorporated in the network by coordination bonds. According to Eq. [1], the reduced product possibly contains a py–S$^-$ moiety, which is coordinated to the cadmium atom. The lower irreversibility, i.e., weak intensity of the reoxidation wave, of **2** is ascribed to the separation of the terminal S$^-$ sites so far apart, in which the pyridine donor site is anchored at the cadmium atom,
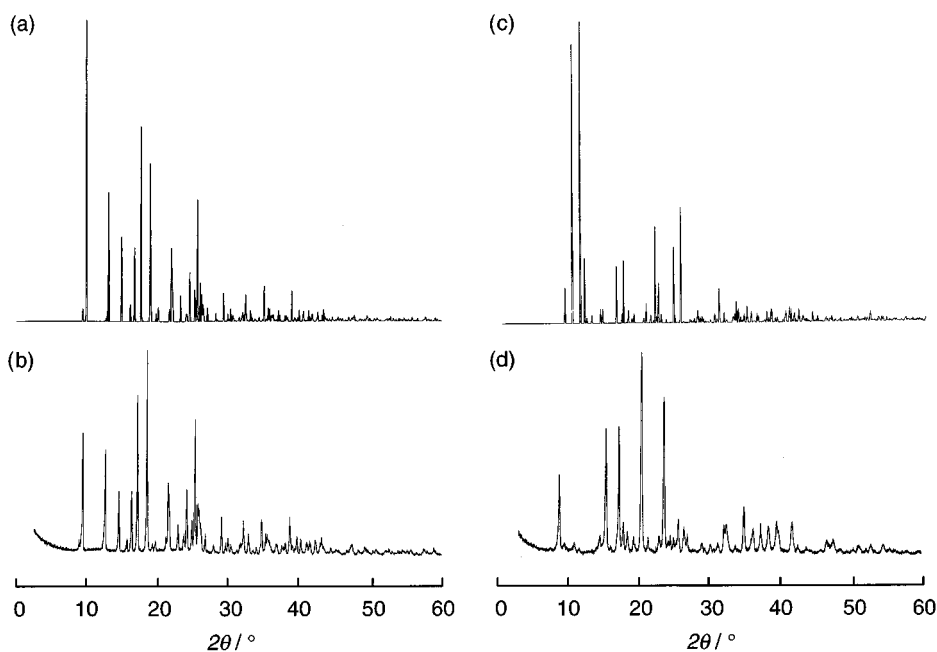

FIG. 3. Simulated (a) and observed (b) XRPD patterns for **1**. Simulated (c) and observed (d) XRPD patterns for **2**.

(a)

1.5   1.0   0.5   0   -0.5   -1.0   -1.5

V vs. SCE

(b)

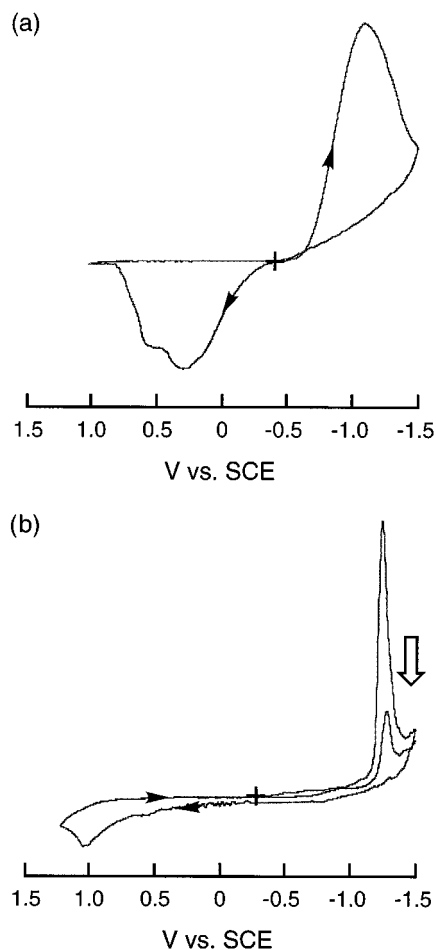1.5   1.0   0.5   0   -0.5   -1.0   -1.5

V vs. SCE

FIG. 4. CV of free dpds (a) and **2** (b) in the solid state.

that the S$^-$ sites hardly recombine for the production of original dpds.

In summary, we demonstrate the synthesis, crystal structures, and redox properties of two coordination network compounds, **1** and **2**·2EtOH·2H$_2$O, from bpe and dpds ligands, respectively. Although their network motifs are similar to each other, **2**·2EtOH·2H$_2$O affords large microchannels, this network is not so robust that the porous network is deformed when the guest molecules are removed. The phase transition was confirmed by XRPD measurements. This coordination network shows a unique redox property based on the disulfide. These results indicate the designed construction for a functional coordination network.

REFERENCES

1. J.-M. Lehn, "Supramolecular Chemistry: Concepts and Perspectives," VCH, Weinheim, 1995.
2. J. C. MacDonald and G. M. Whitesides, *Chem. Rev.* **94,** 2383 (1994).
3. O. M. Yaghi, H. Li, C. Davis, D. Richardson, and T. L. Groy, *Acc. Chem. Res.* **31,** 474 (1998).
4. M. J. Zaworotko, *Chem. Soc. Rev.* 283 (1994).
5. M. J. Zaworotko, *Angew. Chem. Int. Ed. Engl.* **37,** 1211 (1998).
6. M. Munakata, L. P. Wu, and T. Kuroda-Sowa, *Bull. Chem. Soc. Jpn.* **70,** 1727 (1997).
7. S. Kitagawa and M. Kondo, *Bull. Chem. Soc. Jpn.* **71,** 1739 (1998).
8. C. Janiak, *Angew. Chem. Int. Ed. Engl.* **36,** 1431 (1997).
9. O. Kahn, "Molecular Magnetism," VCH, New York, 1993.
10. D. Hagrman, R. P. Hammond, R. Haushalter, and J. Zubieta, *Chem. Mater.* **10,** 2091 (1998).
11. J. S. Müller, A. J. Epstein, and W. M. Reiff, *Chem. Rev.* **88,** 201 (1988).
12. K.-Y. Law, *Chem. Rev.* **93,** 449 (1993).
13. M. Fujita, Y. J. Kwon, S. Washizu, and K. Ogura, *J. Am. Chem. Soc.* **116,** 1151 (1994).
14. D. Venkataraman, G. B. Gardner, S. Lee, and J. S. Moore, *J. Am. Chem. Soc.* **117,** 11600 (1995).
15. H. J. Choi and M. P. Suh, *J. Am. Chem. Soc.* **120,** 10622 (1998).
16. M. Kondo, T. Yoshitomi, K. Seki, H. Matsuzaka, and S. Kitagawa, *Angew. Chem. Int. Ed. Engl.* **36,** 1725 (1997).
17. S. Noro, M. Kondo, S. Kitagawa, T. Ishii, and H. Matsuzaka, *Chem. Lett.* 727 (1999).
18. M. Kondo, T. Okubo, A. Asami, S. Noro, S. Kitagawa, T. Ishii, H. Matsuzaka, and K. Seki, *Angew. Chem. Int. Ed. Engl.* **38,** 140 (1999).
19. M. Kondo, A. Asami, K. Fujimoto, S. Noro, S. Kitagawa, T. Ishii, and H. Matsuzaka, *J. Inorg. Mater.* **1,** 73 (1999).
20. M. Kondo, M. Shimamura, S. Noro, T. Yoshitomi, S. Minakoshi, and S. Kitagawa, *Chem. Lett.* 285 (1999).
21. S. Noro, M. Kondo, T. Ishii, S. Kitagawa, and H. Matsuzaka, *J. Chem. Soc. Dalton Trans.* 1569 (1999).
22. M. Kondo, A. Asami, H. Chang, and S. Kitagawa, *Crystallogr. Eng.* **2,** 115 (1999).
23. M. Fujita, Y. J. Kwon, M. Miyazawa, and K. Ogura, *J. Chem. Soc. Chem. Commun.* 1977 (1994).
24. S. Kitagawa, S. Matsuyama, M. Munakata, N. Osawa, and H. Masuda, *J. Chem. Soc. Dalton Trans.* 1717 (1991).